Automatica 71 (2016) 78–88

Contents lists available at ScienceDirect

Automatica

journal homepage: www.elsevier.com/locate/automatica

Rigid body pose estimation based on the Lagrange–d'Alembert principle☆

Maziar Izadi [a], Amit K. Sanyal [b,1]

[a] Department of Aerospace Engineering, Texas A&M University, College Station, TX 77840, USA
[b] Department of Mechanical and Aerospace Engineering, Syracuse University, Syracuse, NY 13244, USA

ARTICLE INFO

Article history:
Received 18 March 2015
Received in revised form
26 December 2015
Accepted 10 April 2016

Keywords:
Pose estimation
Variational estimator
Lagrange–d'Alembert principle
Lie group variational integrator

ABSTRACT

Stable estimation of rigid body pose and velocities from noisy measurements, without any knowledge of the dynamics model, is treated using the Lagrange–d'Alembert principle from variational mechanics. With body-fixed vision and inertial sensor measurements, a Lagrangian is obtained as the difference between a kinetic energy-like term that is quadratic in velocity estimation error and the sum of two artificial potential functions; one obtained from a generalization of Wahba's function for attitude estimation and another which is quadratic in the position estimate error. An additional dissipation term that is linear in the velocity estimation error is introduced, and the Lagrange–d'Alembert principle is applied to the Lagrangian with this dissipation. A Lyapunov analysis shows that the state estimation scheme so obtained provides stable asymptotic convergence of state estimates to actual states in the absence of measurement noise, with an almost global domain of attraction. This estimation scheme is discretized for computer implementation using discrete variational mechanics, as a first order Lie group variational integrator. The discrete estimation scheme can also estimate velocities from such onboard sensor measurements. Moreover, all states can be estimated during time periods when measurements of only two inertial vectors, the angular velocity vector, and one feature point position vector are available in body frame. In the presence of bounded measurement noise in the vector measurements, numerical simulations show that the estimated states converge to a bounded neighborhood of the true states.

1. Introduction

Estimation of coupled translational and rotational motion is indispensable for operations of spacecraft, unmanned aerial and underwater vehicles. Autonomous state estimation of a rigid body based on inertial vector measurement and visual feedback from stationary landmarks (Karpenko, Konovalenko, Miller, Miller, & Nikolaev, 2015; Miller & Miller, 2015), in the absence of a dynamics model for the rigid body, is analyzed here. The estimation scheme proposed here can also be applied to *relative state* estimation with respect to moving objects (Misra, Izadi, Sanyal, & Scheeres, 2015). This estimation scheme can enhance the autonomy and reliability of unmanned vehicles in uncertain GPS-denied environments. Salient features of this estimation scheme are (1) use of onboard optical and inertial sensors, with or without rate gyros, for autonomous navigation; (2) robustness to uncertainties and lack of knowledge of dynamics; (3) low computational complexity for easy implementation with onboard processors; (4) proven stability with large domain of attraction for state estimation errors; and (5) versatile enough to estimate motion with respect to stationary as well as moving objects. Robust state estimation of rigid bodies in the absence of complete knowledge of their dynamics, is required for their safe, reliable, and autonomous operations in poorly known conditions. In practice, the dynamics of a vehicle may not be perfectly known, especially when the vehicle is under the action of poorly known forces and moments. The scheme proposed here has a single, stable algorithm for the coupled translational and rotational motion of rigid bodies using onboard optical and inertial sensors. This avoids the need for measurements from external sources, like GPS, which may not be available in indoor, underwater or cluttered environments (Amelin & Miller, 2014; Leishman, McLain, & Beard, 2014; Miller & Miller, 2014).

Attitude estimators using unit quaternions for attitude representation may be *unstable in the sense of Lyapunov*, unless

☆ The material in this paper was not presented at any conference. This paper was recommended for publication in revised form by Associate Editor Andrey V. Savkin under the direction of Editor Ian R. Petersen.

E-mail addresses: maziar@tamu.edu (M. Izadi), aksanyal@syr.edu (A.K. Sanyal).
[1] Tel.: +1 315 443 0466.

http://dx.doi.org/10.1016/j.automatica.2016.04.028
0005-1098/

they identify antipodal quaternions with a single attitude. This is also the case for attitude control schemes based on continuous feedback of unit quaternions, as shown in Bayadi and Banavar (2014); Chaturvedi, Sanyal, and McClamroch (2011); Sanyal, Fosbury, Chaturvedi, and Bernstein (2009). One adverse consequence of these unstable estimation and control schemes is that they end up taking longer to converge compared with stable schemes under similar initial conditions and initial transient behavior. Continuous-time attitude observers and filtering schemes on SO(3) and SE(3) have been reported in, e.g., Bonnabel, Martin, and Rouchon (2009); Khosravian, Trumpf, Mahony, and Hamel (2015); Khosravian, Trumpf, Mahony, and Lageman (2015); Mahony, Hamel, and Pflimlin (2008); Maithripala, Berg, and Dayawansa (2004); Markley (2006); Rehbinder and Ghosh (2003); Sanyal, Lee, Leok, and McClamroch (2008); Vasconcelos, Cunha, Silvestre, and Oliveira (2010); Vasconcelos, Silvestre, and Oliveira (2008), including recent stochastic filtering approaches (Barrau & Bonnabel, 2015). These estimators do not suffer from kinematic singularities like estimators using coordinate descriptions of attitude, and they do not suffer from unwinding as they do not use unit quaternions. The maximum likelihood (minimum energy) filtering method of Mortensen (1968) was recently applied to attitude estimation, resulting in a nonlinear attitude estimation scheme that seeks to minimize the stored "energy" in measurement errors (Aguiar & Hespanha, 2006; Zamani, 2013; Zamani, Trumpf, & Mahony, 2013). This scheme is obtained by applying Hamilton–Jacobi–Bellman (HJB) theory (Kirk, 1971) to the state space of attitude motion (Zamani, 2013). Since the HJB equation can only be approximately solved with increasingly unwieldy expressions for higher order approximations, the resulting filter is only "near optimal" up to second order. Unlike approximate or "near optimal" filtering schemes that are not provably stable, the estimation scheme obtained here can be solved exactly and is almost globally asymptotically stable. Moreover, unlike filters based on Kalman filtering, the estimator proposed here does not presume any knowledge of the statistics of the initial state estimate or the sensor noise. Indeed, for vector measurements using optical sensors with limited field-of-view, the probability distribution of measurement noise needs to have compact support, unlike additive Gaussian noise processes that are commonly used.

The variational attitude estimator recently appeared in Izadi and Sanyal (2014); Izadi, Sanyal, Barany, and Viswanathan (2015); Izadi, Sanyal, Samiei, and Viswanathan (2015), where it was shown to be almost globally asymptotically stable. Advantages of this scheme over some commonly used competing schemes are reported in Izadi, Samiei, Sanyal, and Kumar (2015). This paper extends the variational estimation framework to coupled rotational (attitude) and translational motion, as exhibited by maneuvering vehicles like small UAVs. In such applications, designing separate state estimators for the translational and rotational motions may not be effective and may lead to poor navigation. For navigation and tracking the motion of such vehicles, the approach proposed here for robust and stable estimation of the coupled translational and rotational motion will be more effective than de-coupled estimation of translational and rotational motion states. Moreover, like other vision-inertial navigation schemes (Shen, Mulgaonkar, Michael, & Kumar, 2013; Shen, Mulgaonkar, Michael, & Kumar, 2013), the estimation scheme proposed here does not rely on GPS. However, unlike many other vision-inertial estimation schemes, the estimation scheme proposed here can be implemented without any direct velocity measurements. Since rate gyros are usually corrupted by high noise content and bias (Goodarzi, Lee, & Lee, 2013), such a velocity measurement-free scheme can result in fault tolerance in the case of faults with rate gyros. Additionally, this estimation scheme can be extended to relative pose estimation between vehicles from optical measurements, without direct communications or measurements of relative velocities (Misra et al., 2015).

The contents of this article are organized as follows. In Section 2, the problem of motion estimation of a rigid body using onboard optical and inertial sensors and the measurement model is introduced. The rigid body states are related to these measurements. Section 3 introduces artificial energy terms representing the measurement residuals corresponding to the rigid body state estimates. The Lagrange–d'Alembert principle is applied to the Lagrangian constructed from these energy terms with a Rayleigh dissipation term linear in the velocity measurement residual, to give the continuous time state estimator. It is shown that, in the absence of measurement noise, state estimates converge to actual states with asymptotic stability, and the domain of attraction is an open dense subset of the state space. Section 4 provides particular versions of this estimation scheme for the cases when direct velocity measurements are not available and when only angular velocity is directly measured. In Section 5, the variational pose estimator is discretized as a Lie group variational integrator, by applying the discrete Lagrange–d'Alembert principle to discretizations of the Lagrangian and the dissipation term. This estimator is simulated numerically in Section 6, for two cases: the case where at least three beacons are measured at each time instant; and the under-determined case, where occasionally less than three beacons are observed. For these simulations, true states of an aerial vehicle are generated using a given dynamics model. Optical/inertial measurements are generated, assuming bounded noise in sensor readings. Using these measurements, state estimates are shown to converge to a neighborhood of actual states, for both cases simulated. Finally, Section 7 lists the contributions and possible future extensions of the work presented in this paper.

2. Navigation using optical and inertial sensors

Consider a rigid body in spatial (rotational and translational) motion. Onboard estimation of the pose involves assigning a coordinate frame fixed to the vehicle body, and another coordinate frame fixed in space that serves as the inertial frame. Let O denote the observed environment and S denote the body. Let S denote a coordinate frame fixed to S and O be a coordinate frame fixed to O, as shown in Fig. 1. Let $R \in \mathrm{SO}(3)$ denote the rotation matrix from frame S to frame O and b denote the position of origin of S expressed in frame O. The pose (transformation) from body fixed frame S to inertial frame O is then given by

$$\mathsf{g} = \begin{bmatrix} R & b \\ 0 & 1 \end{bmatrix} \in \mathrm{SE}(3). \tag{1}$$

Consider vectors known in the inertial frame O and measured by inertial sensors in the vehicle-fixed frame S; let β be the number of such vectors. In addition, consider position vectors of a few stationary points in the inertial frame O measured by optical sensors in the vehicle-fixed frame S. Velocities of the vehicle may be directly measured or can be estimated by linear filtering of the optical position vector measurements (Izadi et al., 2015). Assume that these optical measurements are available for j points at time t, whose positions are known in frame O as p_j, $j \in \mathcal{J}(t)$, where $\mathcal{J}(t)$ denotes the index set of beacons observed at time t. Note that the observed stationary beacons or landmarks may vary over time due to the vehicle's motion. These points generate $\binom{j}{2}$ unique relative position vectors, which are the vectors connecting any two of these landmarks. When two or more position vectors are optically measured, the number of vector measurements that can be used to estimate attitude is $\binom{j}{2} + \beta$. This number needs to be

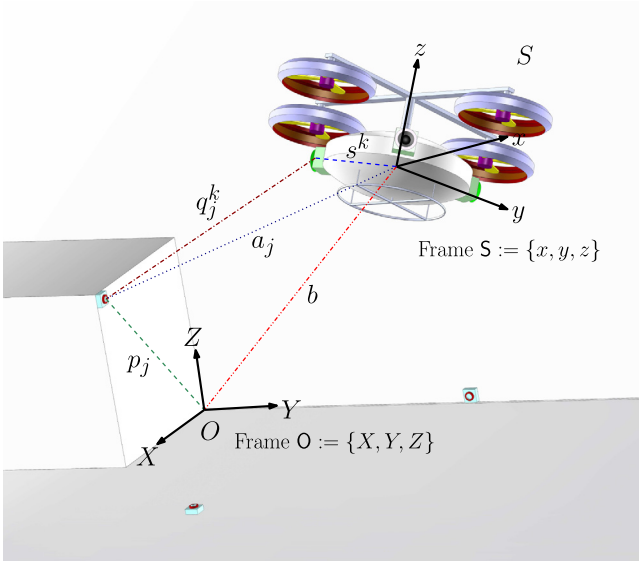

Fig. 1. Inertial landmarks on O as observed from vehicle S with optical measurements.

at least two (i.e., $\binom{j}{2} + \beta \geq 2$) at an instant, for the attitude to be uniquely determined at that instant. In other words, if at least two inertial vectors are measured at all instants (i.e., $\beta \geq 2$), then beacon position measurements are not required for estimating attitude. However, at least one beacon or feature point position measurement is still required to estimate the position of the vehicle. Note that the use of two vector measurements for attitude determination was first proposed by the TRIAD algorithm in the 1960s (Black, 1964).

2.1. Pose measurement model

Denote the position of an optical sensor and the unit vector from that sensor to an observed beacon in frame S as $s^k \in \mathbb{R}^3$ and $u^k \in \mathbb{S}^2$, $k = 1, \ldots, k$, respectively. Denote the relative position of the jth stationary beacon observed by the kth sensor expressed in frame S as q_j^k. Thus, in the absence of measurement noise

$$p_j = R(q_j^k + s^k) + b = Ra_j + b, \quad j \in \mathcal{I}(t), \tag{2}$$

where $a_j = q_j^k + s^k$ are positions of these points expressed in S. In practice, the a_j are obtained from range measurements that have additive noise; we denote as a_j^m the measured vectors. In the case of lidar range measurements, these are given by

$$a_j^m = (q_j^k)^m + s^k = (\varrho_j^k)^m u^k + s^k, \quad j \in \mathcal{I}(t), \tag{3}$$

where $(\varrho_j^k)^m$ is the measured range to the point by the kth sensor. The mean of the vectors p_j and a_j^m are denoted as $\bar{p}$ and $\bar{a}^m$, respectively, and satisfy

$$\bar{a}^m = R^{\mathrm{T}}(\bar{p} - b) + \bar{\zeta}, \tag{4}$$

where $\bar{p} = \frac{1}{j}\sum_{j=1}^{j} p_j$, $\bar{a}^m = \frac{1}{j}\sum_{j=1}^{j} a_j^m$ and $\bar{\zeta}$ is the additive measurement noise obtained by averaging the measurement noise vectors for each of the a_j. Consider the $\binom{j}{2}$ relative position vectors from optical measurements, denoted as $d_j = p_\lambda - p_\ell$ in frame O and the corresponding vectors in frame S as $l_j = a_\lambda - a_\ell$, for $\lambda, \ell \in \mathcal{I}(t)$, $\lambda \neq \ell$. The β measured inertial vectors are included in the set of d_j, and their corresponding measured values expressed in frame S are included in the set of l_j. If the total number of measured vectors (both optical and inertial), $\binom{j}{2} + \beta = 2$, then $l_3 = l_1 \times l_2$ is considered a third measured direction in frame S with corresponding vector $d_3 = d_1 \times d_2$ in frame O. Therefore,

$$d_j = Rl_j \Rightarrow D = RL, \tag{5}$$

where $D = [d_1 \ \ldots \ d_n]$, $L = [l_1 \ \ldots \ l_n] \in \mathbb{R}^{3\times n}$ with $n = 3$ if $\binom{j}{2} + \beta = 2$ and $n = \binom{j}{2} + \beta$ if $\binom{j}{2} + \beta > 2$. Note that the matrix D consists of vectors known in frame O. Denote the measured value of matrix L in the presence of measurement noise as L^m. Then,

$$L^m = R^{\mathrm{T}}D + \mathscr{L}, \tag{6}$$

where $\mathscr{L} \in \mathbb{R}^{3\times n}$ consists of the additive noise in the vector measurements made in the body frame S.

2.2. Velocities measurement model

Denote the angular and translational velocity of the rigid body expressed in body fixed frame S by Ω and ν, respectively. Therefore, the kinematics of the rigid body is

$$\dot{\Omega} = R\Omega^{\times}, \qquad \dot{b} = R\nu \Rightarrow \dot{\mathsf{g}} = \mathsf{g}\xi^{\vee}, \tag{7}$$

where $\xi = \begin{bmatrix}\Omega \\ \nu\end{bmatrix} \in \mathbb{R}^6$ and $\xi^{\vee} = \begin{bmatrix}\Omega^{\times} & \nu \\ 0 & 0\end{bmatrix}$ and $(\cdot)^{\times} : \mathbb{R}^3 \to \mathfrak{so}(3) \subset \mathbb{R}^{3\times 3}$ is the skew-symmetric cross-product operator that gives the vector space isomorphism between $\mathbb{R}^3$ and $\mathfrak{so}(3)$:

$$\chi^{\times} = \begin{bmatrix}\chi_1 \\ \chi_2 \\ \chi_3\end{bmatrix}^{\times} = \begin{bmatrix}0 & -\chi_3 & \chi_2 \\ \chi_3 & 0 & -\chi_1 \\ -\chi_2 & \chi_1 & 0\end{bmatrix}. \tag{8}$$

For the general development of the estimation scheme, it is assumed that the velocities are directly measured. The estimator is then extended to cover the cases where (i) only angular velocity is directly measured; and (ii) none of the velocities are directly measured.

3. Dynamic estimation of motion from proximity measurements

In order to obtain state estimation schemes from measurements as outlined in Section 2 in continuous time, the Lagrange–d'Alembert principle is applied to an action functional of a Lagrangian of the state estimate errors, with a dissipation term linear in the velocities estimate error. This section presents the estimation scheme obtained using this approach. Denote the estimated pose and its kinematics as

$$\hat{\mathsf{g}} = \begin{bmatrix}\hat{R} & \hat{b} \\ 0 & 1\end{bmatrix} \in \mathrm{SE}(3), \qquad \dot{\hat{\mathsf{g}}} = \hat{\mathsf{g}}\hat{\xi}^{\vee}, \tag{9}$$

where $\hat{\xi}$ is rigid body velocities estimate, with $\hat{\mathsf{g}}_0$ as the initial pose estimate. The pose estimation error is

$$\mathsf{h} = \mathsf{g}\hat{\mathsf{g}}^{-1} = \begin{bmatrix}Q & b - Q\hat{b} \\ 0 & 1\end{bmatrix} = \begin{bmatrix}Q & x \\ 0 & 1\end{bmatrix} \in \mathrm{SE}(3), \tag{10}$$

where $Q = R\hat{R}^{\mathrm{T}}$ is the attitude estimation error and $x = b - Q\hat{b}$. Then one obtains, when $\xi^m = \xi$,

$$\dot{\mathsf{h}} = \mathsf{h}\varphi^{\vee}, \quad \text{where } \varphi(\hat{\mathsf{g}}, \xi^m, \hat{\xi}) = \begin{bmatrix}\omega \\ \upsilon\end{bmatrix} = \mathrm{Ad}_{\hat{\mathsf{g}}}(\xi^m - \hat{\xi}), \tag{11}$$

where $\mathrm{Ad}_{\mathscr{g}} = \begin{bmatrix}\mathcal{R} & 0 \\ \mathcal{b}^{\times}\mathcal{R} & \mathcal{R}\end{bmatrix}$ for $\mathscr{g} = \begin{bmatrix}\mathcal{R} & \mathcal{b} \\ 0 & 1\end{bmatrix}$. The attitude and position estimation error dynamics are also in the form

$$\dot{Q} = Q\omega^{\times}, \qquad \dot{x} = Q\upsilon. \tag{12}$$

3.1. Lagrangian from measurement residuals

Consider the sum of rotational and translational measurement residuals between the measurements and estimated pose as a potential energy-like function. Defining the trace inner product on $\mathbb{R}^{n_1\times n_2}$ as

$$\langle A_1, A_2\rangle := \mathrm{trace}(A_1^{\mathrm{T}}A_2), \tag{13}$$

the rotational potential function (Wahba's cost function (Wahba, 1965)) is expressed as

$$\mathcal{U}_r^0(\hat{\mathrm{g}}, L^m, D) = \frac{1}{2}\langle D - \hat{R}L^m, (D-\hat{R}L^m)W\rangle, \tag{14}$$

where $W = \mathrm{diag}(w_j) \in \mathbb{R}^{n\times n}$ is a positive diagonal matrix of weight factors for the measured l_j^m. Consider the translational potential function

$$\mathcal{U}_t(\hat{\mathrm{g}}, \bar{a}^m, \bar{p}) = \frac{1}{2}\kappa y^{\mathrm{T}}y = \frac{1}{2}\kappa\|\bar{p} - \hat{R}\bar{a}^m - \hat{b}\|^2, \tag{15}$$

where $\bar{p}$ is defined by (4), $y \equiv y(\hat{\mathrm{g}}, \bar{a}^m, \bar{p}) = \bar{p} - \hat{R}\bar{a}^m - \hat{b}$ and κ is a positive scalar. Therefore, the total potential function is defined as the sum of the generalization of (14) defined in Izadi and Sanyal (2014); Sanyal, Izadi, and Butcher (2014) for attitude determination on SO(3), and the translational energy (15) as

$$\begin{aligned}\mathcal{U}(\hat{\mathrm{g}}, L^m, D, \bar{a}^m, \bar{p}) &= \mathcal{U}_r(\hat{\mathrm{g}}, L^m, D) + \mathcal{U}_t(\hat{\mathrm{g}}, \bar{a}^m, \bar{p})\\ &= \Phi\big(\mathcal{U}_r^0(\hat{\mathrm{g}}, L^m, D)\big) + \mathcal{U}_t(\hat{\mathrm{g}}, \bar{a}^m, \bar{p})\\ &= \Phi\left(\frac{1}{2}\langle D - \hat{R}L^m, (D-\hat{R}L^m)W\rangle\right)\\ &\quad + \frac{1}{2}\kappa\|\bar{p} - \hat{R}\bar{a}^m - \hat{b}\|^2,\end{aligned} \tag{16}$$

where W is positive definite (not necessarily diagonal), and $\Phi : [0,\infty) \mapsto [0,\infty)$ is a $\mathcal{C}^2$ function that satisfies $\Phi(0) = 0$ and $\Phi'(\chi) > 0$ for all $\chi \in [0,\infty)$. Furthermore, $\Phi'(\cdot) \le \alpha(\cdot)$ where $\alpha(\cdot)$ is a Class-$\mathcal{K}$ function (Khalil, 2001) and $\Phi'(\cdot)$ denotes the derivative of $\Phi(\cdot)$ with respect to its argument. Because of these properties of the function Φ, the critical points and their indices coincide for $\mathcal{U}_r^0$ and $\mathcal{U}_r$ (Izadi & Sanyal, 2014). Define the kinetic energy-like function:

$$\mathcal{T}\Big(\varphi(\hat{\mathrm{g}}, \xi^m, \hat{\xi})\Big) = \frac{1}{2}\varphi(\hat{\mathrm{g}}, \xi^m, \hat{\xi})^{\mathrm{T}}\mathbb{J}\varphi(\hat{\mathrm{g}}, \xi^m, \hat{\xi}), \tag{17}$$

where $\mathbb{J} \in \mathbb{R}^{6\times 6} > 0$ is an artificial inertia-like kernel matrix. Note that in contrast to rigid body inertia matrix, $\mathbb{J}$ is not subject to intrinsic physical constraints like the triangle inequality, which dictates that the sum of any two eigenvalues of the inertia matrix has to be larger than the third. Instead, $\mathbb{J}$ is a gain matrix that can be used to tune the estimator. For notational convenience, $\varphi(\hat{\mathrm{g}}, \xi^m, \hat{\xi})$ is denoted as φ from now on; this quantity is the velocities estimation error in the absence of measurement noise. Now define the Lagrangian

$$\mathcal{L}(\hat{\mathrm{g}}, L^m, D, \bar{a}^m, \bar{p}, \varphi) = \mathcal{T}(\varphi) - \mathcal{U}(\hat{\mathrm{g}}, L^m, D, \bar{a}^m, \bar{p}), \tag{18}$$

and the corresponding action functional over an arbitrary time interval $[t_0, T]$ for $T > 0$,

$$\mathfrak{s}\big(\mathcal{L}(\hat{\mathrm{g}}, L^m, D, \bar{a}^m, \bar{p}, \varphi)\big) = \int_{t_0}^{T}\mathcal{L}(\hat{\mathrm{g}}, L^m, D, \bar{a}^m, \bar{p}, \varphi)\mathrm{d}t, \tag{19}$$

such that $\dot{\hat{\mathrm{g}}} = \hat{\mathrm{g}}(\hat{\xi})^{\vee}$. The following statement gives the form of the Lagrangian when perfect (noise-free) measurements are available, and derives the variational estimator for rigid body pose and velocities.

Lemma 3.1. *In the absence of measurement noise, the Lagrangian is of the form*

$$\mathcal{L}(\mathrm{h}, D, \bar{p}, \varphi) = \frac{1}{2}\varphi^{\mathrm{T}}\mathbb{J}\varphi - \Phi\big(\langle I - Q, K\rangle\big) - \frac{1}{2}\kappa y^{\mathrm{T}}y, \tag{20}$$

where $K = DWD^{\mathrm{T}}$ and $y \equiv y(\mathrm{h}, \bar{p}) = Q^{\mathrm{T}}x + (I - Q^{\mathrm{T}})\bar{p}$.

Proof. Suppose that all the measured states are noise free. Therefore, one can replace $L^m = L$, $\bar{a}^m = \bar{a}$ and $\xi^m = \xi$. The rotational potential function (14) can be replaced by

$$\begin{aligned}\mathcal{U}_r^0(\mathrm{h}, D) &= \frac{1}{2}\langle D - \hat{R}L, (D-\hat{R}L)W\rangle\\ &= \frac{1}{2}\langle I - Q^{\mathrm{T}}, (I-Q^{\mathrm{T}})DWD^{\mathrm{T}}\rangle = \langle I - Q, K\rangle,\end{aligned} \tag{21}$$

since $\hat{R}L = Q^{\mathrm{T}}D$ for the noise-free case. In addition,

$$y(\mathrm{h}, \bar{p}) = \bar{p} - \hat{R}\bar{a} - \hat{b} = Q^{\mathrm{T}}x + (I - Q^{\mathrm{T}})\bar{p}, \tag{22}$$

as $\hat{b} = Q^{\mathrm{T}}(b - x)$. The translational potential function in the absence of measurement noise can be expressed as

$$\mathcal{U}_t(\mathrm{h}, \bar{p}) = \frac{1}{2}\kappa y^{\mathrm{T}}y. \tag{23}$$

Therefore, the total potential energy function is

$$\begin{aligned}\mathcal{U}(\mathrm{h}, D, \bar{p}) &= \mathcal{U}_r(\mathrm{h}, D) + \mathcal{U}_t(\mathrm{h}, \bar{p})\\ &= \Phi\big(\mathcal{U}_r^0(\mathrm{h}, D)\big) + \mathcal{U}_t(\mathrm{h}, \bar{p})\\ &= \Phi\big(\langle I - Q, K\rangle\big) + \frac{1}{2}\kappa y^{\mathrm{T}}y,\end{aligned} \tag{24}$$

and the kinetic energy function is

$$\mathcal{T}(\varphi) = \frac{1}{2}\varphi^{\mathrm{T}}\mathbb{J}\varphi. \tag{25}$$

Substituting (24) and (25) into:

$$\mathcal{L}(\mathrm{h}, D, \bar{p}, \varphi) = \mathcal{T}(\varphi) - \mathcal{U}(\mathrm{h}, D, \bar{p}) \tag{26}$$

gives the Lagrangian (20) for the noise-free case. □

The positive definite weight matrix W can be selected according to Lemma 2.1 of Izadi and Sanyal (2014).

3.2. Variational estimator for pose and velocities

The following statement gives the nonlinear variational estimator obtained by applying the Lagrange–d'Alembert principle to the Lagrangian (18) with a dissipation term linear in the velocities estimation error.

Theorem 3.2. *The nonlinear variational estimator for pose and velocities is given by*

$$\begin{cases}\mathbb{J}\dot{\varphi} &= \mathrm{ad}^*_{\varphi}\mathbb{J}\varphi - Z(\hat{\mathrm{g}}, L^m, D, \bar{a}^m, \bar{p}) - \mathbb{D}\varphi,\\ \dot{\hat{\xi}} &= \dot{\xi}^m - \mathrm{Ad}_{\hat{\mathrm{g}}^{-1}}\dot{\varphi},\\ \dot{\hat{\mathrm{g}}} &= \hat{\mathrm{g}}(\hat{\xi})^{\vee},\end{cases} \tag{27}$$

where $\mathrm{ad}^*_{\zeta} = (\mathrm{ad}_{\zeta})^{\mathrm{T}}$ and ad_{ζ} is defined by

$$\mathrm{ad}_{\zeta} = \begin{bmatrix} w^{\times} & 0\\ v^{\times} & w^{\times}\end{bmatrix} \quad \text{for } \zeta = \begin{bmatrix} w\\ v\end{bmatrix}, \tag{28}$$

and $Z(\hat{\mathrm{g}}, L^m, D, \bar{a}^m, \bar{p})$ is defined by

$$Z(\hat{\mathrm{g}}, L^m, D, \bar{a}^m, \bar{p}) = \begin{bmatrix}\Phi'\Big(\mathcal{U}_r^0(\hat{\mathrm{g}}, L^m, D)\Big)S_{\Gamma}(\hat{R}) + \kappa\bar{p}^{\times}y\\ \kappa y\end{bmatrix}, \tag{29}$$

where $\mathcal{U}_r^0(\hat{\mathrm{g}}, L^m, D)$ *is defined as* (14), $y \equiv y(\hat{\mathrm{g}}, \bar{a}^m, \bar{p}) = \bar{p} - \hat{R}\bar{a}^m - \hat{b}$ *and*

$$S_\Gamma(\hat{R}) = \mathrm{vex}\big(\Gamma\hat{R}^{\mathrm{T}} - \hat{R}\Gamma^{\mathrm{T}}\big) = \mathrm{vex}\big(DW(L^m)^{\mathrm{T}}\hat{R}^{\mathrm{T}} - \hat{R}L^mWD^{\mathrm{T}}\big), \tag{30}$$

$\Gamma = DW(L^m)^{\mathrm{T}}$, $\mathrm{vex}(\cdot) : \mathfrak{so}(3) \to \mathbb{R}^3$ *is the inverse of the* $(\cdot)^\times$ *map, and* $\mathbb{D} \in \mathbb{R}^{6\times 6} > 0$.

Proof. A Rayleigh dissipation term linear in the velocities of the form $\mathbb{D}\varphi$ is used in addition to the Lagrangian (20), and the Lagrange–d'Alembert principle from variational mechanics is applied to obtain the estimator on TSE(3). *Reduced variations* with respect to h and φ (Bloch, 2003; Marsden & Ratiu, 1999) are applied, given by

$$\delta\mathrm{h} = \mathrm{h}\eta^\vee, \qquad \delta\varphi = \dot{\eta} + \mathrm{ad}_\varphi\eta, \quad \text{where } \eta^\vee = \begin{bmatrix} \Sigma^\times & \rho \\ 0 & 0 \end{bmatrix}, \tag{31}$$

for $\eta = \begin{bmatrix} \Sigma \\ \rho \end{bmatrix} \in \mathbb{R}^6$ and $\zeta = \begin{bmatrix} w \\ v \end{bmatrix} \in \mathbb{R}^6$, with $\eta(t_0) = \eta(T) = 0$. This leads to the expression:

$$\delta_{\mathrm{h},\varphi}\mathcal{S}\big(\mathcal{L}(\mathrm{h}, D, \bar{p}, \varphi)\big) = \int_{t_0}^{T} \eta^{\mathrm{T}}\mathbb{D}\varphi\mathrm{d}t. \tag{32}$$

Note that variations of attitude and position estimation errors are of the form

$$\delta Q = Q\Sigma^\times, \qquad \delta x = Q\rho, \tag{33}$$

respectively. Applying reduced variations to the rotational potential energy term (21), one obtains

$$\delta_Q\mathcal{U}_r^0(\mathrm{h}, D) = \langle -Q\Sigma^\times, K\rangle = \frac{1}{2}\langle\Sigma^\times, KQ - Q^{\mathrm{T}}K\rangle = S_K^{\mathrm{T}}(Q)\Sigma, \tag{34}$$

where

$$S_K(Q) = \mathrm{vex}\big(KQ - Q^{\mathrm{T}}K\big). \tag{35}$$

Taking first variation of the translational potential energy term (23) with respect to Q and x yields

$$\delta_{\mathrm{h}}\mathcal{U}_t(\mathrm{h}, \bar{p}) = \kappa(\delta x + \delta Q\bar{p})^{\mathrm{T}}\big\{x + (Q - I)\bar{p}\big\} = \kappa\big(\rho^{\mathrm{T}}y + \Sigma^{\mathrm{T}}\bar{p}^\times y\big). \tag{36}$$

Therefore, the first variation of the total potential energy (24) with respect to estimation errors is

$$\delta_{\mathrm{h}}\mathcal{U}(\mathrm{h}, D, \bar{p}) = Z^{\mathrm{T}}(\mathrm{h}, D, \bar{p})\eta, \tag{37}$$

where $Z(\mathrm{h}, D, \bar{p})$ is defined by

$$Z(\mathrm{h}, D, \bar{p}) = \begin{bmatrix} \Phi'\Big(\langle I - Q, K\rangle\Big)S_K(Q) + \kappa\bar{p}^\times\big\{Q^{\mathrm{T}}x + (I - Q^{\mathrm{T}})\bar{p}\big\} \\ \kappa\{Q^{\mathrm{T}}x + (I - Q^{\mathrm{T}})\bar{p}\} \end{bmatrix}. \tag{38}$$

Taking the first variation of the kinetic energy term (25) with respect to φ results in

$$\delta_\varphi\mathcal{T}(\varphi) = \varphi^{\mathrm{T}}\mathbb{J}\delta\varphi = \varphi^{\mathrm{T}}\mathbb{J}(\dot{\eta} + \mathrm{ad}_\varphi\eta), \tag{39}$$

after substituting Eq. (31). Therefore, the first variation of the action functional (19) is obtained as

$$\begin{aligned}\delta_{\mathrm{h},\varphi}\mathcal{S}\big(\mathcal{L}(\mathrm{h}, D, \bar{p}, \varphi)\big) &= \int_{t_0}^{T}\big\{\varphi^{\mathrm{T}}\mathbb{J}(\dot{\eta} + \mathrm{ad}_\varphi\eta) - \eta^{\mathrm{T}}Z(\mathrm{h}, D, \bar{p})\big\}\mathrm{d}t \\ &= \int_{t_0}^{T}\eta^{\mathrm{T}}\Big(\mathrm{ad}_\varphi^*\mathbb{J}\varphi - Z(\mathrm{h}, D, \bar{p}) - \mathbb{J}\dot{\varphi}\Big)\mathrm{d}t + \varphi^{\mathrm{T}}\mathbb{J}\eta|_{t_0}^{T} \\ &= \int_{t_0}^{T}\eta^{\mathrm{T}}\Big(\mathrm{ad}_\varphi^*\mathbb{J}\varphi - Z(\mathrm{h}, D, \bar{p}) - \mathbb{J}\dot{\varphi}\Big)\mathrm{d}t,\end{aligned} \tag{40}$$

applying fixed endpoint variations with $\eta(t_0) = \eta(T) = 0$. Substituting (40) in expression (32) one obtains

$$\mathbb{J}\dot{\varphi} = \mathrm{ad}_\varphi^*\mathbb{J}\varphi - Z(\mathrm{h}, D, \bar{p}) - \mathbb{D}\varphi, \tag{41}$$

where $Z(\mathrm{h}, D, \bar{p})$ is defined by (38). To implement this estimator in the presence of noisy measurements, substitute $Q^{\mathrm{T}}D = \hat{R}L^m$. This changes the expression for the rotational potential energy from (21) to (14). Eq. (35) is also reformulated as

$$\begin{aligned}S_K(Q) &= \mathrm{vex}(DWD^{\mathrm{T}}Q - Q^{\mathrm{T}}DWD^{\mathrm{T}}) \\ &= \mathrm{vex}(DW(L^m)^{\mathrm{T}}\hat{R}^{\mathrm{T}} - \hat{R}(L^m)WD^{\mathrm{T}}) = S_\Gamma(\hat{R}).\end{aligned} \tag{42}$$

Finally, the second row in the matrix $Z(\mathrm{h}, D, \bar{p})$ is replaced by

$$\begin{aligned}\kappa\{Q^{\mathrm{T}}x + (I - Q^{\mathrm{T}})\bar{p}\} &= \kappa\{Q^{\mathrm{T}}b - \hat{b} + \bar{p} - Q^{\mathrm{T}}\bar{p}\} \\ &= \kappa\{\hat{R}R^{\mathrm{T}}(b - \bar{p}) - \hat{b} + \bar{p}\} \\ &= \kappa\{-\hat{R}\bar{a}^m - \hat{b} + \bar{p}\}.\end{aligned} \tag{43}$$

Taking these changes into account, one obtains the first of Eq. (27) with $Z(\hat{\mathrm{g}}, L^m, D, \bar{a}^m, \bar{p})$ and $S_\Gamma(\hat{R})$ defined by (29) and (30), respectively. Thus, the complete nonlinear estimator equations are given by (27). □

This variational pose estimator uses a fundamentally new idea of applying a principle from variational mechanics to obtain a state estimator, first applied to rigid body attitude estimation in Izadi and Sanyal (2014). In the proposed approach, the time evolution of state estimation errors has the form of the dynamics of a rigid body with Rayleigh dissipation. This results in an estimator for the motion states that dissipates the "energy" content in the estimation errors $(\mathrm{h}, \varphi) = (\mathrm{g}\hat{\mathrm{g}}^{-1}, \mathrm{Ad}_{\hat{\mathrm{g}}}(\xi - \hat{\xi}))$ to provide guaranteed asymptotic stability in the case of perfect measurements (Izadi & Sanyal, 2014). This approach differs from the "minimum-energy" approach to nonlinear estimation (Mortensen, 1968), which applies Hamilton–Jacobi–Bellman (HJB) theory (Kirk, 1971)and can only be "approximately solved." The resulting near-optimal filtering approach was applied to estimation of rigid body attitude and pose in Zamani (2013); Zamani et al. (2013), but has no guarantees on stability. Comparisons between the variational attitude estimator and some commonly-used attitude estimation schemes were detailed in Izadi et al. (2015).

3.3. Stability and robustness of estimator

The stability of the estimator (filter) given by Theorem 3.2 is analyzed here. The following result shows that this scheme is stable, with almost global convergence of the estimated states to the real states.

Theorem 3.3. *Let the observed position vectors from optical measurements be bounded. Then, the estimator presented in Theorem 3.2 is asymptotically stable at the estimation error state* $(\mathrm{h}, \varphi) = (I, 0)$. *Further, the domain of attraction of* $(\mathrm{h}, \varphi) = (I, 0)$ *is a dense open subset of* $\mathrm{SE}(3) \times \mathbb{R}^6$.

The proof of this result is omitted here because it is provided in Misra et al. (2015) for the case of estimation of relative pose and velocities of one body with respect to another. This proof is also similar to the proof of stability of the variational attitude estimator provided in Izadi and Sanyal (2014).

The domain of attraction for $(\mathrm{h}, \varphi) = (I, 0)$ is almost global over the state space $\mathrm{TSE}(3) \simeq \mathrm{SE}(3) \times \mathbb{R}^6$, which is the best possible for continuous control and navigation schemes on a non-contractible state space (Chaturvedi et al., 2011; Milnor, 1963). In the presence of measurement noise with bounded frequencies and amplitudes, one can show that the state estimates converge

to a bounded neighborhood of the true states. The size of this neighborhood depends on the values of the estimator gains $\mathbb{J}$, W and $\mathbb{D}$ and amplitude of noise. These estimator gains can also be designed for desired transient and steady-state behaviors.

Remark 3.4. In the special case that the weight matrix W in Wahba's function is chosen as a piecewise time constant matrix according to Lemma 2.1 of Izadi and Sanyal (2014), $K = DWD^{\mathrm{T}}$ is a constant matrix for all time. Therefore, the RHS of (41) is not explicitly dependent on time. This makes (h, φ) an autonomous system and therefore the use of Theorem 8.4 of Khalil (2001) is not required to prove asymptotic stability. One can apply LaSalle's invariance principle (Theorem 4.4 in Khalil (2001)) to prove the convergence of state estimates to the equilibrium $(I, 0)$ in this case.

This nonlinear estimator combines certain desirable features of stochastic estimation and observer design approaches to state estimation for unmanned vehicles, when inertial vectors and inertially fixed beacons or landmarks are measured. It does not require a dynamics model for the vehicle; instead, it estimates the dynamics of the vehicle given the measurement model in Section 2. The variational pose estimator can also be interpreted as a stable complementary filter (cf. Tayebi, Roberts, and Benallegue (2011)). Explicit expressions for the vector of velocities ξ^m can be obtained for two common cases when these velocities are not directly measured. These two cases are dealt with next.

4. Variational estimator implemented without direct velocity measurements

The velocity measurements in (27) can be replaced by filtered velocity estimates obtained by linear filtering of optical and inertial measurements. This is both useful and necessary when velocities are not directly measured. The filtered values ξ^f are then used in place of ξ^m in the nonlinear estimator given by Theorem 3.2. Denote the measured vector quantity at time t by z^m. A linear second-order filter of the form

$$\ddot{z}^f + 2\mu\omega_n \dot{z}^f = \omega_n^2 \left(z^m - z^f\right), \tag{44}$$

is used, where ω_n is the natural (cutoff) frequency, μ is the damping ratio, and z^f is the filtered value of z^m. Thereafter, z^f is used in place of z^m in Eq. (27).

4.1. Translational and angular velocity measurements are not available

In the case that both angular and translational velocity measurements are not available or accurate, rigid body velocities can be calculated in terms of the inertial and optical measurements. In order to do so, one can differentiate (2) as follows

$$\begin{aligned} &\dot{p}_j = R\Omega^{\times} a_j + R\dot{a}_j + \dot{b} = R\left(\Omega^{\times} a_j + \dot{a}_j + v\right) = 0 \\ \Rightarrow &\dot{a}_j - a_j^{\times}\Omega + v = 0 \\ \Rightarrow &v_j = \dot{a}_j = [a_j^{\times} \quad -I]\xi = G(a_j)\xi, \end{aligned} \tag{45}$$

where $G(a_j) = [a_j^{\times} \quad -I]$ has full row rank. From vision or Doppler lidar sensors, one can also measure the velocities of the observed points in frame S, denoted v_j^m. The measurement model for velocities is of the form

$$v_j^m = G(a_j)\xi + \vartheta_j, \tag{46}$$

where $\vartheta_j \in \mathbb{R}^3$ is the additive error in velocity measurement v_j^m. Instantaneous angular and translational velocity determination from such measurements is treated in Sanyal et al. (2014). Note that $v_j = \dot{a}_j$, for $j \in \mathcal{J}(t)$. As Eq. (45) indicates, the relative velocities of at least three beacons are needed to determine the vehicle's translational and angular velocities uniquely at each instant. However, when only one or two landmarks/beacons are measured, the estimator can propagate velocity estimates based on a least squares determination from available measurements. The rigid body velocities in both cases are obtained using the pseudo-inverse of $\mathbb{G}(A^f)$:

$$\mathbb{G}(A^f)\xi^f = \mathbb{V}(V^f) \Rightarrow \xi^f = \mathbb{G}^{\ddagger}(A^f)\mathbb{V}(V^f), \tag{47}$$

$$\text{where} \quad \mathbb{G}(A^f) = \begin{bmatrix} G(a_1^f) \\ \vdots \\ G(a_j^f) \end{bmatrix} \quad \text{and} \quad \mathbb{V}(V^f) = \begin{bmatrix} v_1^f \\ \vdots \\ v_j^f \end{bmatrix}, \tag{48}$$

for $1, \ldots, j \in \mathcal{J}(t)$. When at least three beacons are measured, $\mathbb{G}(A^f)$ is a full column rank matrix, and $\mathbb{G}^{\ddagger}(A^f) = \left(\mathbb{G}^{\mathrm{T}}(A^f)\mathbb{G}(A^f)\right)^{-1} \mathbb{G}^{\mathrm{T}}(A^f)$ gives its pseudo-inverse. For the case that only one or two beacons are observed, $\mathbb{G}(A^f)$ is a full row rank matrix, whose pseudo-inverse is given by $\mathbb{G}^{\ddagger}(A^f) = \mathbb{G}^{\mathrm{T}}(A^f)\left(\mathbb{G}(A^f)\mathbb{G}^{\mathrm{T}}(A^f)\right)^{-1}$.

4.2. Angular velocity is measured using rate gyros

For the case that rate gyro measurements of angular velocities are available besides the j feature point (or beacon) position measurements, the linear velocities of the rigid body can be calculated using each single position measurement by rewriting (45) as

$$v^f = \sum_{j=1}^{j} (a_j^f)^{\times} \Omega^f - v_j^f, \tag{49}$$

averaging over the j points measured. Averaging the values of v derived from all feature points gives a more reliable result. Therefore, the rigid body's filtered velocities are expressed in this case as

$$\xi^f = \begin{bmatrix} \Omega^f \\ \dfrac{1}{j}\displaystyle\sum_{j=1}^{j} (a_j^f)^{\times}\Omega^f - v_j^f \end{bmatrix}. \tag{50}$$

Remark 4.1. The variational pose estimator of Theorem 3.2 is asymptotically stable, as stated in Theorem 3.3. However, this result may not hold for this estimator with ξ^m replaced by ξ^f as given by Eqs. (47) or (50). In addition, a stochastic interpretation of this estimator in the future could be used to show that the expected values of the state estimates converge to true states if the measurements are unbiased.

5. Discretization for computer implementation

For onboard computer implementation, the continuous time variational estimation scheme has to be discretized. This discretization is carried out in the framework of discrete geometric mechanics, and the resulting discrete-time estimator is in the form of a Lie group variational integrator (LGVI), as in Sanyal et al. (2008). As this estimation scheme is obtained from a variational principle of mechanics, it can be discretized by applying the discrete Lagrange–d'Alembert principle (Marsden & West, 2001). Consider an interval of time $[t_0, T] \in \mathbb{R}^+$ separated into N equal-length subintervals $[t_i, t_{i+1}]$ for $i = 0, 1, \ldots, N$, with $t_N = T$ and $t_{i+1} - t_i = \Delta t$ is the time step size. Let $(\hat{\mathsf{g}}_i, \hat{\xi}_i) \in \mathrm{SE}(3) \times \mathbb{R}^6$ denote the discrete state estimate at time t_i, such that $(\hat{\mathsf{g}}_i, \hat{\xi}_i) \approx (\hat{\mathsf{g}}(t_i), \hat{\xi}(t_i))$ where $(\hat{\mathsf{g}}(t), \hat{\xi}(t))$ is the exact solution of

the continuous-time estimator at time $t \in [t_0, T]$. Let the values of the discrete-time measurements ξ^m, $\bar{a}^m$ and L^m at time t_i be denoted as ξ_i^m, $\bar{a}_i^m$ and L_i^m, respectively. Further, denote the corresponding values of the latter two quantities in inertial frame at time t_i by $\bar{p}_i$ and D_i, respectively. The term representing the energy content of the pose estimation error, given by (16), is discretized as

$$\begin{aligned}\mathcal{U}(\hat{\mathsf{g}}_i, L_i^m, D_i, \bar{a}_i^m, \bar{p}_i) &= \mathcal{U}_r(\hat{\mathsf{g}}_i, L_i^m, D_i) + \mathcal{U}_t(\hat{\mathsf{g}}_i, \bar{a}_i^m, \bar{p}_i)\\ &= \Phi\big(\mathcal{U}_r^0(\hat{\mathsf{g}}_i, L_i^m, D_i)\big) + \mathcal{U}_t(\hat{\mathsf{g}}_i, \bar{a}_i^m, \bar{p}_i)\\ &= \Phi\big(\frac{1}{2}\langle D_i - \hat{R}_i L_i^m, (D_i - \hat{R}_i L_i^m) W_i\rangle\big)\\ &\quad + \frac{1}{2}\kappa\|\bar{p}_i - \hat{R}_i\bar{a}_i^m - \hat{b}_i\|^2, \end{aligned} \tag{51}$$

where W_i is the matrix of weight factors corresponding to D_i. The term encapsulating the energy in the velocities estimate error (17), is discretized as

$$\mathcal{T}\Big(\varphi(\hat{\mathsf{g}}_i, \xi_i^m, \hat{\xi}_i)\Big) = \frac{1}{2}\varphi(\hat{\mathsf{g}}_i, \xi_i^m, \hat{\xi}_i)^{\mathrm{T}}\mathbb{J}\varphi(\hat{\mathsf{g}}_i, \xi_i^m, \hat{\xi}_i), \tag{52}$$

where $\mathbb{J} = \text{blockdiag}(J, M)$ and $M, J \in \mathbb{R}^{3\times 3}$ are positive definite.

Lemma 5.1. *In the absence of measurement noise, the discrete-time Lagrangian is of the form*

$$\begin{aligned}\mathcal{L}(\mathsf{h}_i, D_i, \bar{p}_i, \varphi_i) &= \frac{1}{2}\langle \mathcal{J}\omega_i^\times, \omega_i^\times\rangle + \frac{1}{2}\langle M\upsilon_i, \upsilon_i\rangle\\ &\quad - \Phi\big(\langle I - Q_i, K_i\rangle\big) - \frac{1}{2}\kappa y_i^{\mathrm{T}} y_i,\end{aligned} \tag{53}$$

where $y_i \equiv y(\mathsf{h}_i, \bar{p}_i) = Q_i^{\mathrm{T}} x_i + (I - Q_i^{\mathrm{T}})\bar{p}_i$ *and* $\mathcal{J}$ *is defined in terms of the matrix* J *by* $\mathcal{J} = \frac{1}{2}\text{trace}[J]I - J$.

A Lie group variational integrator (LGVI) introduced in Sanyal, Nordkvist, and Chyba (2011) is applied to the discrete-time Lagrangian (53) to obtain the discrete-time estimator. The value of the total energy function corresponding to this discrete-time Lagrangian can be shown to decrease with time.

Theorem 5.2. *A discrete-time variational estimator corresponding to the continuous-time estimator proposed in Theorem 3.2 is*

$$(J\omega_i)^\times = \frac{1}{\Delta t}(F_i\mathcal{J} - \mathcal{J}F_i^{\mathrm{T}}), \tag{54}$$

$$\begin{aligned}(M + \Delta t\mathbb{D}_t)\upsilon_{i+1} &= F_i^{\mathrm{T}} M\upsilon_i\\ &\quad + \Delta t\kappa(\hat{b}_{i+1} + \hat{R}_{i+1}\bar{a}_{i+1}^m - \bar{p}_{i+1}),\end{aligned} \tag{55}$$

$$\begin{aligned}(J + \Delta t\mathbb{D}_r)\omega_{i+1} &= F_i^{\mathrm{T}} J\omega_i + \Delta t M\upsilon_{i+1}\times\upsilon_{i+1}\\ &\quad + \Delta t\kappa\bar{p}_{i+1}^\times(\hat{b}_{i+1} + \hat{R}_{i+1}\bar{a}_{i+1}^m)\\ &\quad - \Delta t\Phi'\big(\mathcal{U}_r^0(\hat{\mathsf{g}}_{i+1}, L_{i+1}^m, D_{i+1})\big)S_{\Gamma_{i+1}}(\hat{R}_{i+1}),\end{aligned} \tag{56}$$

$$\hat{\xi}_i = \xi_i^m - \text{Ad}_{\hat{\mathsf{g}}_i^{-1}}\varphi_i, \tag{57}$$

$$\hat{\mathsf{g}}_{i+1} = \hat{\mathsf{g}}_i\exp(\Delta t\hat{\xi}_i^\vee), \tag{58}$$

where $F_i \in \text{SO}(3)$, $\big(\hat{\mathsf{g}}(t_0), \hat{\xi}(t_0)\big) = (\hat{\mathsf{g}}_0, \hat{\xi}_0)$, $\varphi_i = [\omega_i^{\mathrm{T}}\ \upsilon_i^{\mathrm{T}}]^{\mathrm{T}}$, *and* $S_{\Gamma_i}(\hat{R}_i)$ *is the value of* $S_\Gamma(\hat{R})$ *at time* t_i, *with* $S_\Gamma(\hat{R})$ *as defined by* (30).

Proof. Consider the first variations with fixed endpoints for the pose estimation errors in discrete time:

$$\delta Q_i = Q_i\Sigma_i^\times, \qquad \Sigma_0 = \Sigma_N = 0, \tag{59}$$

$$\delta x_i = Q_i\rho_i, \qquad \rho_0 = \rho_N = 0, \tag{60}$$

where $\Sigma_i, \rho_i \in \mathbb{R}^3$ are "discrete variation vectors". It can be shown that for any $\omega \in \mathbb{R}^3$ we have

$$(J\omega)^\times = \omega^\times\mathcal{J} + \mathcal{J}\omega^\times. \tag{61}$$

Discretizing (12) assuming that the angular velocity estimation error is constant in the time interval $[t_i, t_{i+1}]$ with a constant time step size Δt, one gets

$$Q_{i+1} = Q_i F_i, \quad i \in \{0, 1, 2, \ldots, N-1\}, \tag{62}$$

where $F_i \in \text{SO}(3)$ is given by

$$F_i = \exp(\Delta t\omega_i^\times) \approx I + \Delta t\omega_i^\times. \tag{63}$$

The variation of F_i is derived from (62) and $\delta Q_i = Q_i\Sigma_i^\times$:

$$\delta F_i = -\Sigma_i^\times F_i + F_i\Sigma_{i+1}^\times. \tag{64}$$

Using (61) and (63), one can approximate $(J\omega_i)^\times$ as

$$\begin{aligned}(J\omega_i)^\times &= \omega_i^\times\mathcal{J} + \mathcal{J}\omega_i^\times \approx \frac{1}{\Delta t}\Big((F_i - I)\mathcal{J} - \mathcal{J}(F_i^{\mathrm{T}} - I)\Big)\\ &= \frac{1}{\Delta t}(F_i\mathcal{J} - \mathcal{J}F_i^{\mathrm{T}}).\end{aligned} \tag{65}$$

From (11), the continuous kinematics of the position estimation error is discretized to first order as

$$\frac{x_{i+1} - x_i}{\Delta t} \approx Q_i\upsilon_i \Rightarrow x_{i+1} = \Delta t Q_i\upsilon_i + x_i. \tag{66}$$

The first variation in υ_i is then calculated from (66) as

$$\begin{aligned}\delta\upsilon_i &= \delta\Big(\frac{1}{\Delta t}Q_i^{\mathrm{T}}(x_{i+1} - x_i)\Big)\\ &= -\Sigma_i^\times\upsilon_i + \frac{1}{\Delta t}Q_i^{\mathrm{T}}(\delta x_{i+1} - \delta x_i)\\ &= -\Sigma_i^\times\upsilon_i + \frac{1}{\Delta t}F_i\rho_{i+1} - \frac{1}{\Delta t}\rho_i.\end{aligned} \tag{67}$$

The discrete Lagrangian (53) can be expressed as

$$\begin{aligned}\mathcal{L}(\mathsf{h}_i, D_i, \bar{p}_i, F_i, \upsilon_i) &= \frac{1}{2\Delta t}\langle\mathcal{J}(F_i - I), (F_i - I)\rangle\\ &\quad + \frac{\Delta t}{2}\langle M\upsilon_i, \upsilon_i\rangle - \Delta t\Phi\big(\mathcal{U}_r^0(\mathsf{h}_i, D_i)\big)\\ &\quad - \frac{\Delta t}{2}\kappa(Q_i y_i)^{\mathrm{T}}(Q_i y_i).\end{aligned} \tag{68}$$

The action functional (19) is replaced by the action sum

$$\mathcal{S}_d\big(\mathcal{L}(\mathsf{h}_i, D_i, \bar{p}_i, F_i, \upsilon_i)\big) = \Delta t\sum_{i=0}^{N-1}\mathcal{L}(\mathsf{h}_i, D_i, \bar{p}_i, F_i, \upsilon_i). \tag{69}$$

Applying the discrete Lagrange–d'Alembert principle with two Rayleigh dissipation terms for angular and translational motions gives

$$\begin{aligned}&\delta\mathcal{S}_d\big(\mathcal{L}(\mathsf{h}_i, D_i, \bar{p}_i, F_i, \upsilon_i)\big)\\ &\quad + \Delta t\sum_{i=0}^{N-1}\Big\{\langle\Sigma_i, \tau_i\rangle + \langle\rho_i, f_i\rangle\Big\} = 0\\ &\Rightarrow\sum_{i=0}^{N-1}\Big\{\frac{1}{\Delta t}\langle\delta F_i, \mathcal{J}(F_i - I)\rangle + \Delta t\langle\delta\upsilon_i, M\upsilon_i\rangle\\ &-\frac{\Delta t}{2}\Phi'\big(\mathcal{U}_r^0(\mathsf{h}_i, D_i)\big)\big\langle\Sigma_i^\times, S_{K_i}^\times(Q_i)\big\rangle - \Delta t\kappa\langle\rho_i, y_i\rangle\\ &-\Delta t\kappa\langle\Sigma_i^\times, y_i\bar{p}_i^{\mathrm{T}}\rangle + \frac{\Delta t}{2}\langle\Sigma_i^\times, \tau_i^\times\rangle + \Delta t\langle\rho_i, f_i\rangle\Big\} = 0.\end{aligned} \tag{70}$$

As symmetric matrices are orthogonal to skew-symmetric matrices in the trace inner product, using (63) the first term in (68) is expressed as

$$\begin{aligned}\langle\delta F_i, \mathcal{J}(F_i - I)\rangle &= \langle\Sigma_i^\times, \mathcal{J}F_i^{\mathrm{T}}\rangle - \langle\Sigma_{i+1}^\times, F_i^{\mathrm{T}}\mathcal{J}\rangle\\ &= \frac{1}{2}\langle\Sigma_i^\times, \mathcal{J}F_i^{\mathrm{T}}\rangle - \frac{1}{2}\langle\Sigma_i^\times, F_i\mathcal{J}\rangle\end{aligned} \tag{71}$$

$$-\frac{1}{2}\langle \Sigma_{i+1}^{\times}, F_i^{\mathrm{T}}\mathcal{J}\rangle + \frac{1}{2}\langle \Sigma_{i+1}^{\times}, \mathcal{J}F_i\rangle$$
$$=-\frac{\Delta t}{2}\langle \Sigma_i^{\times}, (J\omega_i)^{\times}\rangle + \frac{\Delta t}{2}\langle \Sigma_{i+1}^{\times}, F_i^{\mathrm{T}}(J\omega_i)^{\times}F_i\rangle.$$

Hence Eq. (70) can be re-expressed as

$$\sum_{i=0}^{N-1}\Bigg\{-\frac{1}{2}\langle \Sigma_i^{\times}, (J\omega_i)^{\times}\rangle + \frac{1}{2}\langle \Sigma_{i+1}^{\times}, F_i^{\mathrm{T}}(J\omega_i)^{\times}F_i\rangle$$
$$-\frac{\Delta t}{2}\langle \Sigma_i^{\times}, (\upsilon_i\times M\upsilon_i)^{\times}\rangle + \langle F_i\rho_{i+1}, M\upsilon_i\rangle$$
$$-\langle \rho_i, M\upsilon_i\rangle - \frac{\Delta t}{2}\Phi'\big(\mathcal{U}_r^0(\mathsf{h}_i, D_i)\big)\big\langle \Sigma_i^{\times}, S_{K_i}^{\times}(Q_i)\big\rangle$$
$$-\kappa\Delta t\langle \rho_i, y_i\rangle - \frac{\kappa\Delta t}{2}\big\langle \Sigma_i^{\times}, (\bar{p}_i^{\times}y_i)^{\times}\big\rangle$$
$$+\frac{\Delta t}{2}\langle \Sigma_i^{\times}, \tau_i^{\times}\rangle + \Delta t\langle \rho_i, f_i\rangle\Bigg\} = 0. \tag{72}$$

Separating this equation into two (rotational and translational) parts leads to

$$(M+\Delta t\mathbb{D}_t)\upsilon_{i+1} = F_i^{\mathrm{T}}M\upsilon_i - \Delta t\kappa y_{i+1}, \tag{73}$$

$$(J+\Delta t\mathbb{D}_r)\omega_{i+1} = F_i^{\mathrm{T}}J\omega_i + \Delta t M\upsilon_{i+1}\times\upsilon_{i+1} - \Delta t\kappa\bar{p}_{i+1}^{\times}y_{i+1} - \Delta t\Phi'\big(\mathcal{U}_r^0(\mathsf{h}_{i+1}, D_{i+1})\big)S_{K_{i+1}}(Q_{i+1}), \tag{74}$$

using the identity $\mathcal{F}^{\mathrm{T}}w^{\times}\mathcal{F} = (\mathcal{F}^{\mathrm{T}}w)^{\times}$ and substituting $\tau_i = -\mathbb{D}_r\omega_i$ and $f_i = -\mathbb{D}_t\upsilon_i$, where $\mathbb{D}_r$ and $\mathbb{D}_t$ are positive definite matrices such that

$$\mathbb{D} = \begin{bmatrix}\mathbb{D}_r & 0\\ 0 & \mathbb{D}_t\end{bmatrix}.$$

In the presence of measurement noise, $Q_i^{\mathrm{T}}D_i$ and y_i are replaced by $\hat{R}_iL_i^m$ and $\bar{p}_i-\hat{b}_i-\hat{R}_i\bar{a}_i^m$, respectively. This results in the discrete-time state estimator in the form of the Lie group variational integrator (54)–(58). □

Note that unlike the dynamics model-based discrete-time rigid body state estimators using LGVI schemes in Sanyal et al. (2008); Sanyal and Nordkvist (2012), the above is a model-free state estimator like the recent ones in Izadi and Sanyal (2014); Izadi et al. (2015).

Remark 5.3. In the absence of any velocity measurements or only angular velocity measurements, the expressions provided in Section 4 to calculate rigid body velocities are still valid in discrete-time. One can use the discrete-time variables introduced in this section in place of their continuous-time counterparts. The second-order Butterworth filter (44) is discretized using the *Newmark-β Method* as

$$\begin{cases} z_{i+1}^f = z_i^f + \Delta t\,\dot{z}_i^f + \dfrac{\Delta t^2}{4}(\ddot{z}_i^f + \ddot{z}_{i+1}^f)\\ \dot{z}_{i+1}^f = \dot{z}_i^f + \dfrac{\Delta t}{2}(\ddot{z}_i^f + \ddot{z}_{i+1}^f).\end{cases} \tag{75}$$

This method gives the filtered positions and velocities as

$$\begin{Bmatrix} z_{i+1}^f\\ \dot{z}_{i+1}^f\end{Bmatrix} = \frac{1}{4+4\mu\omega_n\Delta t+\omega_n^2\Delta t^2}\begin{bmatrix}4+4\mu\omega_n\Delta t-\omega_n^2\Delta t^2 & 4\Delta t & \omega_n^2\Delta t^2\\ -4\omega_n^2\Delta t & 4-4\mu\omega_n\Delta t-\omega_n^2\Delta t^2 & 2\omega_n^2\Delta t\end{bmatrix}\begin{Bmatrix} z_i^f\\ \dot{z}_i^f\\ z_i^m + z_{i+1}^m\end{Bmatrix}, \tag{76}$$

where $z_i^m = z^m(t_i)$ and $z_i^f = z^f(t_i)$, respectively. As with the continuous time version, ξ_i^m can be replaced with ξ_i^f in the estimator equations.

6. Numerical simulations

This section presents numerical simulation results for the discrete-time estimator obtained in Section 5. In order to numerically simulate this estimator, simulated true states of an aerial vehicle flying in a room are produced using the kinematics and dynamics equations of a rigid body. The vehicle mass and moment of inertia are taken to be $m_v = 420$ g and $J_v = [51.2 \quad 60.2 \quad 59.6]^{\mathrm{T}}$ g m^2, respectively. The resultant external forces and torques applied on the vehicle are $\phi_v(t) = 10^{-3}[10\cos(0.1t) \quad 2\sin(0.2t) \quad -2\sin(0.5t)]^{\mathrm{T}}$ N and $\tau_v(t) = 10^{-6}\phi_v(t)$ N.m, respectively. The room is assumed to be a cubic space of size 10 m × 10 m × 10 m with the inertial frame origin at the center of this cube. The initial attitude and position of the vehicle are

$$R_0 = \mathrm{expm}_{\mathrm{SO(3)}}\left(\left(\frac{\pi}{4}\times\begin{bmatrix}\frac{3}{7} & -\frac{6}{7} & \frac{2}{7}\end{bmatrix}^{\mathrm{T}}\right)^{\times}\right),$$
$$\text{and } b_0 = [2.5 \;\; 0.5 \;\; -3]^{\mathrm{T}}\ \text{m}. \tag{77}$$

This vehicle's initial angular and translational velocities, respectively, are

$$\Omega_0 = [0.2 \;\; -0.05 \;\; 0.1]^{\mathrm{T}}\ \text{rad/s},$$
$$\text{and } \nu_0 = [-0.05 \;\; 0.15 \;\; 0.03]^{\mathrm{T}}\ \text{m/s}. \tag{78}$$

The vehicle dynamics is simulated over a time interval of $T = 150$ s, with a time stepsize of $\Delta t = 0.02$ s. The trajectory of the vehicle over this time interval is depicted in Fig. 2. The following two inertial directions, corresponding to nadir and Earth's magnetic field direction, are measured by the inertial sensors on the vehicle:

$$d_1 = [0 \;\; 0 \;\; -1]^{\mathrm{T}}, \qquad d_2 = [0.1 \;\; 0.975 \;\; -0.2]^{\mathrm{T}}. \tag{79}$$

For optical measurements, eight beacons are located at the eight vertices of the cube, labeled 1–8. The positions of these beacons are known in the inertial frame and their index (label) and relative positions are measured by optical sensors onboard the vehicle whenever the beacons come into the field of view of the sensors. Three identical cameras (optical sensors) and inertial sensors are assumed to be installed on the vehicle. The cameras are fixed to known positions on the vehicle, on a hypothetical horizontal plane passing through the vehicle, 120° apart from each other, as shown in Fig. 1. All camera readings contain random zero mean signals whose probability distributions are normalized bump functions with width of 0.5°. The filtered velocities are obtained using Eq. (47). The following are selected for the positive definite estimator gain matrices:

$$J = \mathrm{diag}\big([0.9 \;\; 0.6 \;\; 0.3]\big),$$
$$M = \mathrm{diag}\big([0.0608 \;\; 0.0486 \;\; 0.0365]\big),$$
$$\mathbb{D}_r = \mathrm{diag}\big([2.7 \;\; 2.2 \;\; 1.5]\big), \qquad \mathbb{D}_t = \mathrm{diag}\big([0.1 \;\; 0.12 \;\; 0.14]\big). \tag{80}$$

For simplicity, the function $\Phi(\cdot)$ is selected to be $\Phi(x) = x$. The initial state estimates have the following values:

$$\hat{\mathfrak{g}}_0 = I, \quad \hat{\Omega}_0 = [0.1 \;\; 0.45 \;\; 0.05]^{\mathrm{T}}\ \text{rad/s},$$
$$\text{and } \hat{\nu}_0 = [2.05 \;\; 0.64 \;\; 1.29]^{\mathrm{T}}\ \text{m/s}. \tag{81}$$

The performance of the proposed estimator is presented for two different cases.

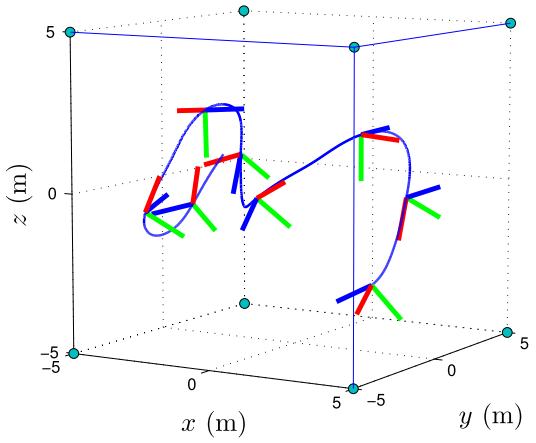

Fig. 2. Position and attitude trajectory of the simulated vehicle in 3D space.

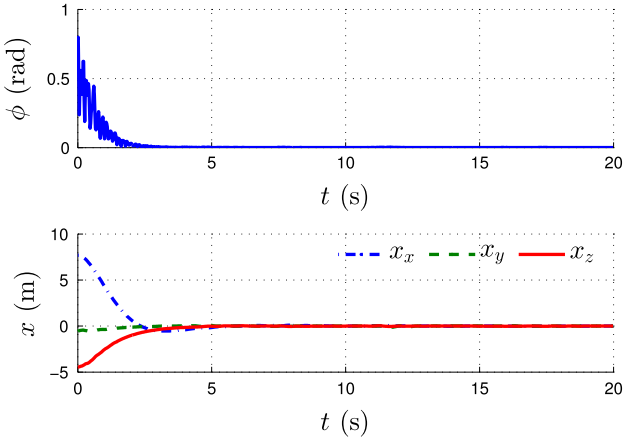

Fig. 3. Principal angle of the attitude and position estimation error for CASE 1.

6.1. CASE 1: At least three beacons are observed at each time instant

Having three beacons measured at each time guarantees full determination of vehicle's instantaneous translational and angular velocities. A conic field of view (FOV) of $2^\circ \times 40^\circ$ for cameras satisfies this condition for the given volume. The discrete-time estimator (54)–(58) is simulated over a time interval of $T = 20$ s with sampling interval $\Delta t = 0.02$ s. At each time instant, (54) is solved using Newton–Raphson iterations. Following this, the remaining equations (all explicit) are solved for the state estimates. The principal angle of the attitude estimation error and the position estimation error for CASE 1 are plotted in Fig. 3. Plots of the angular and translational velocity estimation errors are shown in Fig. 4.

6.2. CASE 2: Less than three beacons are measured at some time instants

To implement the variational estimator for the case that less than three optical measurements are available, the field of view of the cameras is decreased to limit the number of beacons observed. Assuming the cameras have conical fields of view of $2^\circ \times 25^\circ$, the minimum number of beacons observed instantaneously drops to one during the simulated time interval. The true dynamics of the aerial vehicle, simulated time duration, and sample rate are identical to CASE 1. Fig. 5 depicts the principal angle of the attitude estimation error and the position estimation error for CASE 2, and Fig. 6 shows the angular and translational velocity estimation errors. All estimation errors are shown to converge to a neighborhood of $(\mathrm{h}, \varphi) = (I, 0)$ in both cases.

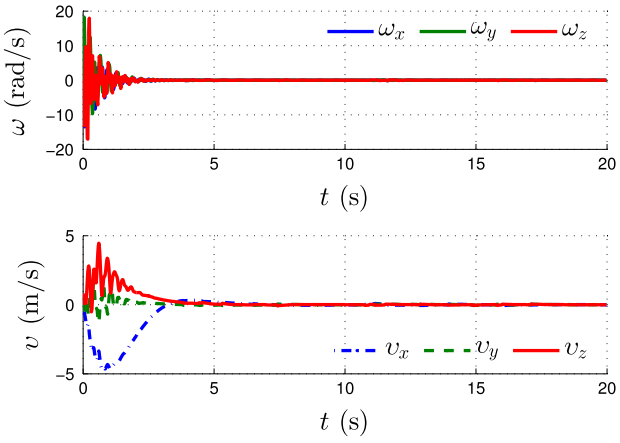

Fig. 4. Angular and translational velocity estimation error for CASE 1.

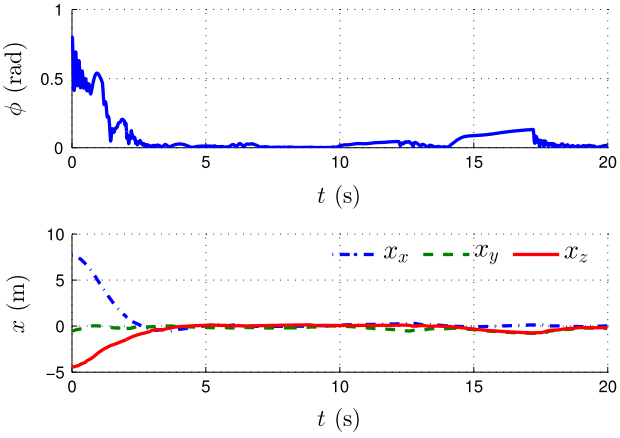

Fig. 5. Principal angle of the attitude and position estimation error for CASE 2.

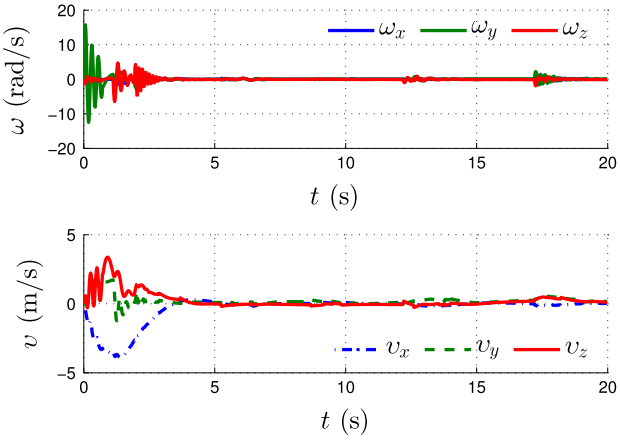

Fig. 6. Angular and translational velocity estimation error for CASE 2.

7. Conclusion

This article proposes an estimator for rigid body pose and velocities, using optical and inertial measurements by onboard sensors. The sensors are assumed to provide (possibly noisy) measurements in continuous-time or at a sufficiently high frequency. An artificial kinetic energy quadratic in rigid body velocity estimate errors is defined, as well as two fictitious potential energies: (1) a generalization of Wahba's cost function for attitude estimation error, and (2) a quadratic function of the vehicle's position

estimate error. Applying the Lagrange–d'Alembert principle to a Lagrangian consisting of these energy-like terms and a dissipation term linear in velocities estimation error, an estimator is designed on the Lie group of rigid body motions. This estimator is shown to be almost globally asymptotically stable, with estimates converging to actual states in a domain of attraction that is open and dense in the state space. The continuous estimator is discretized applying the discrete Lagrange–d'Alembert principle to the discrete Lagrangian and dissipation terms linear in rotational and translational velocity estimation errors. In the presence of measurement noise, numerical simulations show that state estimates converge to a bounded neighborhood of the true states. Future extensions of this work include higher-order discretizations of the continuous-time filter given here, extending the variational estimation framework with dissipation to other mechanical systems, and obtaining a stochastic interpretation of this variational pose estimator.

References

Aguiar, A., & Hespanha, J. (2006). Minimum-energy state estimation for systems with perspective outputs. *IEEE Transactions on Automatic Control*, *51*(2), 226–241.

Amelin, K. S., & Miller, A. B. (2014). An algorithm for refinement of the position of a light UAV on the basis of Kalman filtering of bearing measurements. *Journal of Communications Technology and Electronics*, *59*(6), 622–631.

Barrau, A., & Bonnabel, S. (2015). An intrinsic Cramér-Rao bound on SO(3) for (dynamic) attitude filtering. In *Proceedings of the IEEE conference on decision and control*, Osaka, Japan (pp. 2158–2163).

Bayadi, R., & Banavar, R. N. (2014). Almost global attitude stabilization of a rigid body for both internal and external actuation schemes. *European Journal of Control*, *20*(1), 45–54.

Black, H. (1964). A passive system for determining the attitude of a satellite. *American Institute of Aeronautics and Astronautics*, *2*(7), 1350–1351.

Bloch, A. M. (2003). *Nonholonomic mechanics and control*. New York: Springer-Verlag.

Bonnabel, S., Martin, P., & Rouchon, P. (2009). Nonlinear symmetry-preserving observers on lie groups. *IEEE Transactions on Automatic Control*, *54*(7), 1709–1713.

Chaturvedi, N. A., Sanyal, A. K., & McClamroch, N. H. (2011). Rigid-body attitude control. *IEEE Control Systems Magazine*, *31*(3), 30–51.

Goodarzi, F., Lee, D., & Lee, T. (2013). Geometric nonlinear PID control of a quadrotor UAV on SE(3.) In *Proceedings of the European control conference*, Zurich, Switzerland (pp. 3845–3850).

Izadi, M., Samiei, E., Sanyal, A. K., & Kumar, V. (2015). Comparison of an attitude estimator based on the Lagrange-d'Alembert principle with some state-of-the-art filters. In *Proceedings of the IEEE international conference on robotics and automation*, Seattle, WA, USA (pp. 2848–2853).

Izadi, M., & Sanyal, A. K. (2014). Rigid body attitude estimation based on the lagrange-d'alembert principle. *Automatica*, *50*(10), 2570–2577.

Izadi, M., Sanyal, A. K., Barany, E., & Viswanathan, S. P. (2015). Rigid body motion estimation based on the Lagrange-d'Alembert principle. In *Proceedings of the 54nd IEEE conference on decision and control*, Osaka, Japan.

Izadi, M., Sanyal, A. K., Samiei, E., & Viswanathan, S. P. (2015). Discrete-time rigid body attitude state estimation based on the discrete Lagrange-d'Alembert principle. In *Proceedings of the American control conference*, Chicago, IL, USA (pp. 3392–3397).

Karpenko, S., Konovalenko, I., Miller, A., Miller, B., & Nikolaev, D. (2015). UAV control on the basis of 3d landmarks bearing-only observations. *Sensors*, *15*(12), 29802–29820.

Khalil, H. K. (2001). *Nonlinear systems* (3rd ed.). Prentice Hall: Upper Saddle River, NJ.

Khosravian, A., Trumpf, J., Mahony, R., & Hamel, T. (2015). Recursive attitude estimation in the presence of multi-rate and multi-delay vector measurements. In *Proceedings of the American control conference*, Chicago, IL, USA (pp. 3199–3205).

Khosravian, A., Trumpf, J., Mahony, R., & Lageman, C. (2015). Observers for invariant systems on lie groups with biased input measurements and homogeneous outputs. *Automatica*, *55*, 19–26.

Kirk, D. E. (1971). *Optimal control theory: an introduction*. NY: Prentice Hall.

Leishman, R. C., McLain, T. W., & Beard, R. W. (2014). Relative navigation approach for vision-based aerial gps-denied navigation. *Journal of Intelligent and Robotic Systems*, *74*(1–2), 97–111.

Mahony, R., Hamel, T., & Pflimlin, J. M. (2008). Nonlinear complementary filters on the special orthogonal group. *IEEE Transactions on Automatic Control*, *53*(5), 1203–1218.

Maithripala, D.H., Berg, J.M., & Dayawansa, W.P. (2004). An intrinsic observer for a class of simple mechanical systems on a Lie group. In *Proceedings of the American control conference*, Boston, MA, USA (pp. 1546–1551).

Markley, F. L. (2006). Attitude filtering on so(3). *The Journal of the Astronautical Sciences*, *54*(4), 391–413.

Marsden, J. E., & Ratiu, T. S. (1999). *Introduction to mechanics and symmetry: a basic exposition of classical mechanical systems*. Springer Science & Business Media, *Vol. 17*.

Marsden, J. E., & West, M. (2001). Discrete mechanics and variational integrators. *Acta Numerica*, *10*, 357–514.

Miller, A., & Miller, B. (2014). Tracking of the UAV trajectory on the basis of bearing-only observations. In *Proceedings of the 53rd annual conference on decision and control*, Los Angeles, CA, USA (pp. 4178–4184).

Miller, A., & Miller, B. (2015). Stochastic control of light UAV at landing with the aid of bearing-only observations. In *Proceedings of the 8th international conference on machine vision*, Barcelona, Spain (pp. 987529–987529).

Milnor, J. (1963). *Morse theory*. Princeton, NJ: Princeton University Press.

Misra, G., Izadi, M., Sanyal, A. K., & Scheeres, D. J. (2015). Coupled orbit-attitude dynamics and relative state estimation of spacecraft near small Solar System bodies. *Advances in Space Research*,.

Mortensen, R. E. (1968). Maximum-likelihood recursive nonlinear filtering. *Journal of Optimization Theory and Applications*, *2*(6), 386–394.

Rehbinder, H., & Ghosh, B. K. (2003). Pose estimation using line-based dynamic vision and inertial sensors. *IEEE Transactions on Automatic Control*, *48*(2), 186–199.

Sanyal, A. K., Fosbury, A., Chaturvedi, N. A., & Bernstein, D. S. (2009). Inertia-free spacecraft attitude tracking with disturbance rejection and almost global stabilization. *Journal of Guidance, Control, and Dynamics*, *32*(4), 1167–1178.

Sanyal, A. K., Izadi, M., & Butcher, E. A. (2014). Determination of relative motion of a space object from simultaneous measurements of range and range rate. In *Proceedings of the American Control Conference*, Portland, OR, USA (pp. 1607–1612).

Sanyal, A. K., Lee, T., Leok, M., & McClamroch, N. H. (2008). Global optimal attitude estimation using uncertainty ellipsoids. *Systems & Control Letters*, *57*(3), 236–245.

Sanyal, A. K., & Nordkvist, N. (2012). Attitude state estimation with multi-rate measurements for almost global attitude feedback tracking. *AIAA Journal of Guidance, Control, and Dynamics*, *35*(3), 868–880.

Sanyal, A. K., Nordkvist, N., & Chyba, M. (2011). An almost global tracking control scheme for maneuverable autonomous vehicles and its discretization. *IEEE Transactions on Automatic Control*, *56*(2), 457–462.

Shen, S., Mulgaonkar, Y., Michael, N., & Kumar, V. (2013). Vision-based state estimation and trajectory control towards aggressive flight with a quadrotor. In *Proceedings of the robotics science and systems*.

Shen, S., Mulgaonkar, Y., Michael, N., & Kumar, V. (2013). Vision-based state estimation for autonomous rotorcraft MAVs in complex environments. In *Proceedings of the IEEE international conference on robotics and automation*, Karlsruhe, Germany (pp. 1758–1764).

Tayebi, A., Roberts, A., & Benallegue, A. (2011). Inertial measurements based dynamic attitude estimation and velocity-free attitude stabilization. In *Proceedings of the american control conference*, San Francisco, CA, USA (pp. 1027–1032).

Vasconcelos, J. F., Cunha, R., Silvestre, C., & Oliveira, P. (2010). A nonlinear position and attitude observer on se(3) using landmark measurements. *Systems & Control Letters*, *59*, 155–166.

Vasconcelos, J.F., Silvestre, C., & Oliveira, P. (2008). A nonlinear GPS/IMU based observer for rigid body attitude and position estimation. In *Proceedings of the IEEE conference on decision and control*, Cancun, Mexico (pp. 1255–1260).

Wahba, G. (1965). A least squares estimate of satellite attitude, problem 65-1. *SIAM Review*, *7*(5), 409.

Zamani, M. (2013). *Deterministic attitude and pose filtering, an embedded Lie groups approach*. (Ph.D. dissertation), Canberra, Australia: Australian National University.

Zamani, M., Trumpf, J., & Mahony, R. (2013). Minimum-energy filtering for attitude estimation. *IEEE Transactions on Automatic Control*, *58*(11), 2917–2921.

Maziar Izadi received his B.Sc. (2007) and M.Sc. (2010) degrees, both in mechanical engineering, from Amirkabir University of Technology (Tehran Polytechnic) and University of Tehran, respectively. He received his Ph.D. degree in mechanical engineering from New Mexico State University in 2015. He is currently a postdoctoral research associate in aerospace engineering at Texas A&M University. His research interests include multibody dynamics, geometric mechanics, state estimation, nonlinear systems and their stability analyses.

Amit K. Sanyal received a B.Tech. in aerospace engineering from the Indian Institute of Technology, Kanpur, in 1999 and M.S. in aerospace engineering from Texas A&M University in 2001. He received the M.S. in mathematics and Ph.D. in aerospace engineering from the University of Michigan in 2004. From 2004 to 2006, he was a postdoctoral research associate in the mechanical and aerospace engineering department at Arizona State University. From 2007 to 2010, he was an assistant professor in mechanical engineering at the University of Hawaii, and from 2010 to 2015 he was in the mechanical and aerospace engineering department at New Mexico State University. He is

currently an associate professor in mechanical and aerospace engineering at Syracuse University. His research interests are in geometric mechanics, geometric control, discrete variational mechanics for numerical integration of mechanical systems, optimal control and estimation, geometric/algebraic methods applied to nonlinear systems, spacecraft guidance and control, and control of unmanned vehicles. He is a member of the IEEE Control Systems Society technical committees on Aerospace Control and Nonlinear Control, and past member of the AIAA Guidance, Navigation, and Control Technical Committee.